Pulmonary Leptospirosis With Diffuse Alveolar Hemorrhage: High-Resolution Computed Tomographic Findings in 16 Patients

Felipe Mussi von Ranke, MD, Gláucia Zanetti, MD, PhD,* Dante Luiz Escuissato, MD, PhD,† Bruno Hochhegger, MD, PhD,*‡ and Edson Marchiori, MD, PhD**

Objective: The aim of this study was to evaluate the high-resolution computed tomographic (HRCT) findings from patients with leptospirosis and diffuse alveolar hemorrhage (DAH).

Materials and Methods: We retrospectively reviewed HRCT findings from 16 patients diagnosed as having leptospirosis causing DAH. The patient sample was composed of 13 men and 3 women aged 22 to 53 years (mean age, 34.5 years). Diagnosis was established with confirmation of leptospirosis infection by serologic microagglutination test. Histopathological study was performed in 8 patients. Two chest radiologists analyzed the HRCT images and reached decisions by consensus.

Results: The predominant HRCT findings were ground-glass opacities and airspace nodules (both n = 12, 75%), ground-glass nodules (n = 9, 56.25%), consolidations (n = 7, 43.75%), "crazy-paving" pattern (n = 3, 18.75%), and interlobular septal thickening without ground-glass opacity (n = 3, 18.75%). Bilateral pleural effusion was an associated finding in 2 (12.5%) patients. Analysis of the axial distribution of the lesions revealed diffuse distribution in 11 (68.75%) patients and peripheral lung zone predominance in 5 (31.25%) patients. Abnormalities were bilateral in all 16 (100%) patients. Analysis of the craniocaudal distribution of the lesions revealed lower zone predominance in 9 (56.25%) patients, diffuse distribution in 5 (31.25%) patients, middle zone predominance in 1 (6.25%) patient, and upper zone predominance in 1 (6.25%) patient.

Conclusions: The most frequent HRCT findings in patients with leptospirosis causing DAH were ground-glass opacities, airspace nodules, ground-glass nodules, and consolidations. The lesions showed symmetrical distribution with lower zone predominance in most cases.

Key Words: leptospirosis, pulmonary hemorrhage, computed tomography

(*J Comput Assist Tomogr* 2016;40: 91–95)

Leptospirosis is a zoonosis caused by spirochetes of the species *Leptospira interrogans*, comprising all human pathogenic strains (>200 serovars). It occurs worldwide, commonly in tropical and subtropical regions, and is one of the most widespread zoonoses in the world, being considered an important public health problem.[1–3] Humans are infected when mucous membranes or abraded skin come into direct contact with the urine of wild or domestic infected animals (especially rats, mice, and dogs) or by exposure to contaminated water or soil or other matter.[1,4]

The diagnosis of leptospirosis is based on clinical findings, history of direct or indirect exposure to infected animals in endemic areas, especially in the context of urban floods or other immersion in contaminated water, and positive serological tests, preferably a microscopic agglutination test.[1,5,6]

Leptospirosis produces numerous clinical findings, but patients usually manifest 2 main clinical presentations. The mild form (anicteric leptospirosis) accounts for 90% of cases and commonly begins abruptly and includes headache, myalgia (especially of the calf muscles), ocular abnormalities, fever, nausea, vomiting, rash, epistaxis, and meningismus. The more severe form (icteric leptospirosis or Weil disease) is associated with jaundice, liver and renal impairment, and major hemorrhagic complications.[4,7–10] Leptospirosis is also associated with cardiovascular collapse and significant mortality.[9]

Severe pulmonary involvement in leptospirosis consists primarily of hemorrhagic pneumonitis. In advanced cases, adult respiratory distress syndrome, diffuse alveolar hemorrhage (DAH), and significant mortality may occur.[1,8,9] The syndrome of DAH consists of hemoptysis, anemia, bilateral airspace opacification on chest radiographs, and a decreased hematocrit secondary to bleeding from the pulmonary microvasculature into the alveolar space.[2,9,11,12]

Although high-resolution computed tomography (HRCT) is superior to chest radiography for the demonstration of subtle features, such as ground-glass opacities, and the extent of abnormalities, few English-language articles have described the tomographic findings of leptospirosis.[1,2,7–10,13,14] Pulmonary infections, particularly leptospirosis, are frequently absent from differential diagnoses in reviews of DAH.[15–17] However, they should be considered because of the obvious therapeutic implications.[2] The aim of this study was to describe HRCT findings from 16 immunocompetent patients with leptospirosis causing DAH.

METHODS

Our institutional review board approved this study and waived the requirement for informed patient consent. All data used in this study were anonymized. This retrospective observational study reviewed HRCT images from 16 patients (13 men, 3 women with a mean age of 34.5 [range, 22–53] years) diagnosed as having leptospirosis and DAH. The patients were examined between 2007 and 2014 in 6 tertiary hospitals in 3 states of Brazil.

The study population was composed of immunocompetent patients with histories of exposure to the risk of acquiring leptospirosis, characteristic signs and symptoms, pulmonary involvement, and diagnoses of leptospirosis infection, regardless of age or sex. The inclusion criteria were diagnostic confirmation of leptospirosis infection by serologic microagglutination test, confirmation of DAH by clinical findings and sequential bronchoalveolar lavage (BAL) revealing increasing red blood cell counts, and availability of chest HRCT images acquired during the acute phase of the disease. Histopathological correlation was performed for 8 patients, who presented intra-alveolar red blood cells with accumulation of siderophages. Patients with other pulmonary infections,

From the*Department of Radiology, Rio de Janeiro Federal University, Rio de Janeiro; †Department of Radiology, Federal University of Paraná, Curitiba; and ‡Department of Radiology, Federal University of Health Sciences of Porto Alegre, Porto Alegre, Brazil.

Received for publication May 4, 2015; accepted July 20, 2015.

Correspondence to: Edson Marchiori, MD, PhD, Rua Thomaz Cameron, 438, Valparaiso, CEP 25685.120, Petrópolis, Rio de Janeiro, Brazil (e-mail: edmarchiori@gmail.com).

The authors declare no conflict of interest.

DOI: 10.1097/RCT.0000000000000318

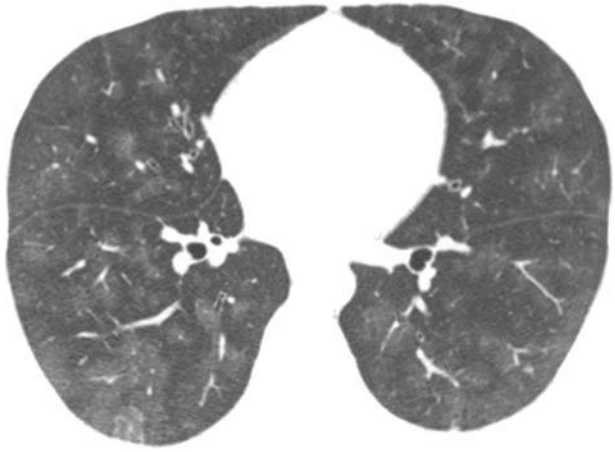

FIGURE 1. A 22-year-old man with leptospirosis. High-resolution CT at the level of the lower lung fields shows bilateral ground-glass opacities.

confirmed by laboratory tests, were excluded, as were those with tomographic findings suggestive of pulmonary involvement resulting from chronic lung diseases.

All HRCT images were obtained 2 to 7 days after the onset of pulmonary symptoms. Chest CT examinations were performed using a variety of helical scanners because different hospitals were involved in this study. In the initial studies, HRCT images were obtained at full inspiration with 1- to 2-mm slice thickness at 5- to 10-mm intervals and reconstructed using a high–spatial frequency reconstruction algorithm. The most recent CT images were obtained using helical acquisition and reconstructed with 1- to 2-mm slice thickness and 1- to 2-mm intervals using a high–spatial frequency reconstruction algorithm. The acquisition time was 0.5 to 1 second per rotation, peak voltage was 120 kVp, modulated tube current was 100 to 400 mA, pitch was 1, and matrix was 512 × 512 pixels. The images were reviewed using mediastinal (width, 350–450 HU; level, 10–20 HU) and lung (width, 1200–1600 HU; level, 2500–2700 HU) window settings.

Two chest radiologists with more than 15 years of experience independently reviewed the images, and final assessment was achieved by consensus. The radiologists were blinded to patient demographics, clinical data, and final diagnoses. The HRCT images were evaluated to determine the presence and distribution of ground-glass opacities, consolidation, airspace or ground-glass nodules, "crazy-paving" pattern, interlobular septal thickening, and any associated findings, such as pleural effusion.

The definition of HRCT findings followed the Glossary of Terms for Thoracic Imaging proposed by the Fleischner Society.[18] Ground-glass opacities appear as hazy increased opacity of the lung, with preservation of bronchial and vascular margins. "Consolidation" was defined as an opacity that obscured the margins of vessels and airway walls, with or without air bronchograms. A "nodule" was defined as a rounded or irregular opacity that was well or poorly defined and 3 cm or less in diameter. Airspace (acinar) nodules are round or ovoid poorly defined pulmonary opacities approximately 5 to 8 mm in diameter. A "ground-glass nodule" was defined as a nodule that did not obliterate the bronchial and vascular margins. Crazy-paving pattern appears as thickened interlobular septa and intralobular lines superimposed on a background of ground-glass opacity. Interlobular septal thickening is seen as thickening of the linear opacities between secondary pulmonary lobules composed of connective tissue and containing lymphatic vessels and pulmonary venules.

The distribution of lesions in the lung parenchyma along the axial axis was classified as central, peripheral, or diffuse. In addition, the predominance of findings in 1 lung or symmetric involvement was recorded. The distribution was noted to be peripheral when abnormalities were predominant in the outer third of the lung periphery, in contact with the pleural surface, and central when abnormalities were predominant in the inner two thirds of the transverse plane. In the craniocaudal direction, lung zones were defined as upper, middle, and lower. The "upper zone" was defined as that above the level of the aortic arch, the "middle zone" was delineated between the aortic arch and carina, and the "lower zone" was defined as that below the level of the carina. Lymph node enlargement and pleural effusions were also assessed.

RESULTS

The most common HRCT findings in our study sample were ground-glass opacities and airspace nodules (Figs. 1–3), observed in 12 (75%) patients each, followed by ground-glass nodules (n = 9, 56.25%) (Fig. 4), consolidations (n = 7, 43.75%) (Fig. 5), crazy-paving pattern (n = 3, 18.75%) (Fig. 6), and interlobular septal thickening without ground-glass opacity (n = 3, 18.75%). Bilateral pleural effusion was observed as an associated finding in 2 (12.5%) patients. A summary of the HRCT findings is presented in Table 1.

Abnormalities were distributed diffusely in 11 (68.75%) patients, and peripheral lung zone predominance was observed in 5 (31.25%) patients. No central lung zone predominance was observed. Abnormalities were bilateral in all 16 (100%) patients, but right lung predominance was observed in 6 (37.5%) patients. Regarding craniocaudal distribution, the lesions demonstrated lower zone predominance in 9 (56.25%) patients, diffuse distribution in 5 (31.25%) patients, middle zone predominance in 1 (6.25%) patient, and upper zone predominance in 1 (6.25%) patient.

DISCUSSION

In our study sample, the most common HRCT findings of DAH caused by leptospirosis were ground-glass opacities and airspace nodules, observed in 12 patients each. Other frequent findings were ground-glass nodules (n = 9), consolidations (n = 7), crazy-paving pattern (n = 3), and interlobular septal thickening without ground-glass opacity (n = 3). Bilateral pleural effusion was seen in 2 patients. Abnormalities were distributed diffusely in 11 patients. The craniocaudal distribution of lesions in our

FIGURE 2. A 48-year-old man with leptospirosis. Computed tomography shows bilateral ground-glass opacities involving mainly the peripheral regions of both lungs.

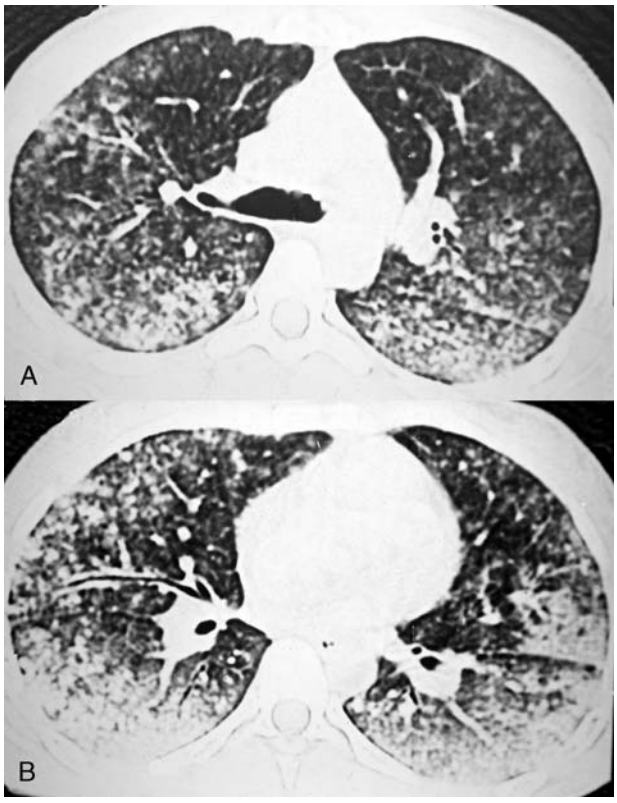

FIGURE 3. A 31-year-old man with leptospirosis. Computed tomography shows bilateral airspace nodules and airspace consolidation involving mainly the subpleural regions.

study revealed lower zone predominance in the majority of (n = 9) patients.

Correlation between HRCT and histopathological findings demonstrated that the areas of ground-glass attenuation and consolidation were represented by filling of alveoli by edema and hemorrhagic exudates. In some cases, the ground-glass pattern reflected the presence of alveolar septal thickening caused by inflammation, with or without airspace filling. The interlobular septal thickening was related to infiltration of the interlobular septa by edema or blood. The airspace nodules were characterized microscopically by alveoli filled with blood.

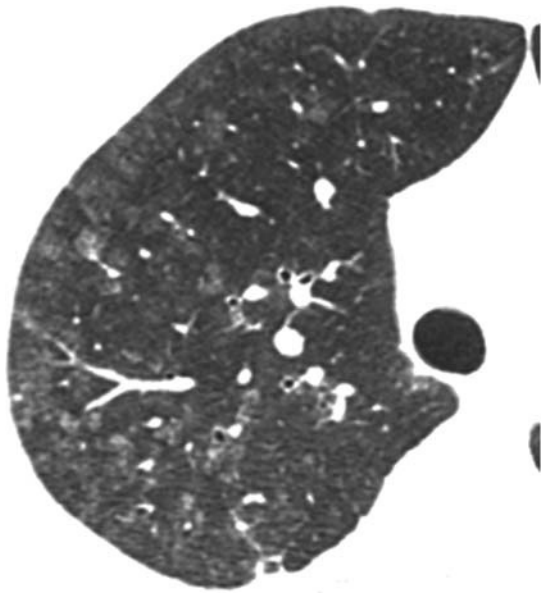

FIGURE 4. A 53-year-old man with leptospirosis. High-resolution CT (right lung) demonstrates disseminated ground-glass nodules in the upper lobe.

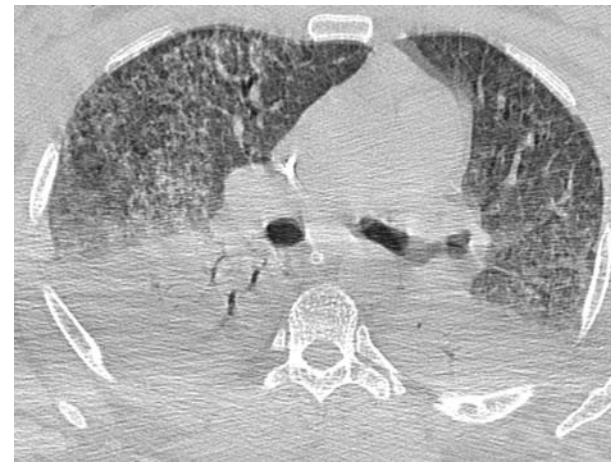

FIGURE 5. A 35-year-old man with leptospirosis. Computed tomography shows bilateral areas of consolidation in the lower lobes, with air bronchogram. Note also ground-glass opacities in both lungs.

The HRCT findings of DAH in leptospirosis reported in the literature are similar to ours. Ground-glass opacities are the most common pattern, frequently involving multiple lobules. Other described findings are ground-glass or airspace nodules, areas of consolidation, and crazy-paving pattern. Abnormalities involve mainly the peripheral and dorsal lung regions and the lower lung zones.[1,2,8,13] The HRCT shows more extensive abnormalities than do chest radiographs. Ground-glass opacities, airspace consolidation, and airspace nodules are caused by pulmonary hemorrhage, as confirmed in BAL and autopsy studies.[1,4,13]

The main route of infection in our casuistic was through contact with flood water (14 patients). The other 2 patients (sewer

FIGURE 6. A 44-year-old man with leptospirosis. High-resolution CT at the level of the lower lobes demonstrates bilateral areas of ground-glass attenuation with superimposed interlobular septal thickening (crazy-paving pattern).

TABLE 1. High-Resolution CT Findings in Patients With Leptospirosis

Finding	n (%)
Ground-glass opacities	12 (75)
Airspace nodules	12 (75)
Ground-glass nodules	9 (56.25)
Consolidations	7 (43.75)
Crazy-paving pattern	3 (18.75)
Interlobular septal thickening without ground-glass opacity	3 (18.75)
Bilateral pleural effusion	2 (12.5)

maintenance workers) had occupational exposure to contaminated water. The disease incubation phase (interval between possible infection and symptom onset) ranged from 7 to 15 days. All patients complained of the sudden onset of headache and fever, with temperatures ranging from 38°C to 40°C. Fourteen patients had myalgia, mainly involving the calves. Progressive dyspnea and crackles on auscultation were observed in 15 cases, with progressive worsening in 9 cases. Hemoptysis was observed in 16 patients and was massive in 7 cases.

Acute renal failure requiring dialysis occurred in 10 patients. Nine of them died. Eight of the 9 patients who died had massive hemoptysis, and 7 evolved with jaundice on hospitalization days 3 to 5. All patients developed respiratory failure and acute respiratory distress syndrome. In the 9 patients who died, worsening of clinical conditions was rapidly progressive. Chest radiographs obtained in the intensive care unit showed increased opacification of the lungs. Seven patients showed progressive clinical improvement and were discharged 10 to 20 days after the onset of pulmonary symptoms. Chest radiographs were obtained for 5 of these patients, and follow-up HRCT was performed for 2 patients, which showed partial reabsorption of pulmonary opacities at a mean interval of 5 days.

Severe forms of leptospirosis are associated with a fatality rate of more than 50%,[19] caused mainly by pulmonary hemorrhage.[4] In 1 series of 89 fatal cases of leptospirosis, pulmonary involvement was detected clinically in 74% of cases and was the strongest risk factor for death. Autopsy was performed in 43 of these patients and showed pulmonary hemorrhage in 72% of cases.[19]

Increased frequency of alveolar infiltrates, dyspnea, and radiological score severity are poor prognostic indicators in severe leptospirosis.[4] Microscopic examination usually demonstrates multiple foci of interstitial and alveolar hemorrhage, with varying degrees of severity. Other findings, such as pulmonary congestion, pulmonary edema, and hyaline membrane formation, are also frequent.[4,20–22] Leptospira are uncommon in the lung tissue, although leptospiral antigen is present at sites of tissue injury. Inflammatory infiltrates are generally not prominent.[4,20,21,23]

Pulmonary hemorrhage may also be occult, with few or no chest radiographic abnormalities despite the presence of clinical symptoms. In a study conducted by Paganin et al,[24] chest radiographs were normal in 38.7% of 31 patients with DAH confirmed by BAL. The HRCT revealed ground-glass opacities consistent with alveolar hemorrhage in these patients.

Our study has some limitations. First, the study was retrospective, limiting the ability to investigate clinical correlations. Second, the HRCT techniques varied widely, given the long (7-year) study period and the different institutions involved in the survey. However, we do not believe that this variation affected our results. Despite these limitations, to our knowledge, this is the first original article systematically addressing the findings of leptospirosis causing DAH evaluated by HRCT.

In conclusion, leptospirosis should be considered in the differential diagnosis of DAH, particularly in regions known to be endemic for the disease. The most frequent patterns observed in immunocompetent patients with leptospirosis causing DAH are ground-glass opacities and airspace nodules. Consolidations, crazy-paving pattern, and ground-glass nodules were also observed. The lesions showed diffuse and symmetrical distribution, with lower zone predominance in most cases.

REFERENCES

1. Marchiori E, Lourenço S, Setúbal S, et al. Clinical and imaging manifestations of hemorrhagic pulmonary leptospirosis: a state-of-the-art review. *Lung*. 2011;189:1–9.
2. von Ranke F, Zanetti G, Hochhegger B, et al. Infectious diseases causing diffuse alveolar hemorrhage in immunocompetent patients: a state-of-the-art review. *Lung*. 2013;191:9–18.
3. Farr RW. Leptospirosis. *Clin Infect Dis*. 1995;21:1–6.
4. Dolhnikoff M, Mauad T, Bethlem EP, et al. Pathology and pathophysiology of pulmonary manifestations in leptospirosis. *Braz J Infect Dis*. 2007;11: 142–148.
5. Castro JR, Salaberry SR, Souza MA, et al. Predominant Leptospira spp. serovars in serological diagnosis of canines and humans in the City of Uberlândia, State of Minas Gerais, Brazil. *Rev Soc Bras Med Trop*. 2011; 44:217–222.
6. Dassanayake DL, Wimalaratna H, Agampodi SB, et al. Evaluation of surveillance case definition in the diagnosis of leptospirosis, using the microscopic agglutination test: a validation study. *BMC Infect Dis*. 2009;9:48.
7. Hashimoto T, Akata S, Park J, et al. High-resolution computed tomography findings in a case of severe leptospira infection (Weil disease) complicated with Jarisch-Herxheimer reaction. *J Thorac Imaging*. 2012; 27:W24–W26.
8. Kishimoto M, Brown JD, Chung HH, et al. Leptospirosis misdiagnosed as pulmonary-renal syndrome. *Am J Med Sci*. 2004;328:116–120.
9. Luks AM, Lakshminarayanan S, Hirschmann JV. Leptospirosis presenting as diffuse alveolar hemorrhage: case report and literature review. *Chest*. 2003;123:639–643.
10. Ketai L, Currie BJ, Alva Lopez LF. Thoracic radiology of infections emerging after natural disasters. *J Thorac Imaging*. 2006;21: 265–275.
11. Ioachimescu OC, Stoller JK. Diffuse alveolar hemorrhage: diagnosing it and finding the cause. *Cleve Clin J Med*. 2008;75:258–265.
12. Fontenot AP, Schwarz MI. Diffuse alveolar hemorrhage. *Interstitial Lung Dis*. 2003;3:632–656.
13. Marchiori E, Müller NL. Leptospirosis of the lung: high-resolution computed tomography findings in five patients. *J Thorac Imaging*. 2002; 17:151–153.
14. Yiu MW, Ooi GC, Yuen KY, et al. High resolution CT of Weil's disease. *Lancet*. 2003;362:117.
15. Lara AR, Schwarz MI. Diffuse alveolar hemorrhage. *Chest*. 2010;137: 1164–1171.
16. Collard HR, Schwarz MI. Diffuse alveolar hemorrhage. *Clin Chest Med*. 2004;25:583–592.
17. Primack SL, Miller RR, Müller NL. Diffuse pulmonary hemorrhage: clinical, pathologic, and imaging features. *AJR Am J Roentgenol*. 1995; 164:295–300.
18. Hansell DM, Bankier AA, MacMahon H, et al. Fleischner Society: glossary of terms for thoracic imaging. *Radiology*. 2008;246: 697–722.

19. Spichler AS, Vilaça PJ, Athanazio DA, et al. Predictors of lethality in severe leptospirosis in urban Brazil. *Am J Trop Med Hyg*. 2008;79: 911–914.

20. Arean VM. The pathologic anatomy and pathogenesis of fatal human leptospirosis (Weil's disease). *Am J Pathol*. 1962;40: 393–423.

21. Nicodemo AC, Duarte MI, Alves VA, et al. Lung lesions in human leptospirosis: microscopic, immunohistochemical, and ultrastructural features related to thrombocytopenia. *Am J Trop Med Hyg*. 1997; 56:181–187.

22. Teglia OF, Battagliotti C, Villavicencio RL, et al. Leptospiral pneumonia. *Chest*. 1995;108:874–875.

23. Nally JE, Chantranuwat C, Wu XY, et al. Alveolar septal deposition of immunoglobulin and complement parallels pulmonary hemorrhage in a guinea pig model of severe pulmonary leptospirosis. *Am J Pathol*. 2004; 164:1115–1127.

24. Paganin F, Bourdin A, Dalban C, et al. Leptospirosis in Reunion Island (Indian Ocean): analysis of factors associated with severity in 147 confirmed cases. *Intensive Care Med*. 2007;33: 1959–1966.